Malaysian Journal of Chemistry, 2024, Vol. 26(3), 320-329
(Special Issue: *3rd Virtual International Symposium on Sciences 2023*)

Spectrophotometric Detection of Fe^{3+} Ion Based on Alizarin Red S (ARS) Reagent

Nurul Atirah Zulkefli and Wan Elina Faradilla Wan Khalid*
School of Chemistry and Environment, Faculty of Applied Sciences,
Universiti Teknologi MARA, Cawangan Negeri Sembilan, Kampus Kuala Pilah, 72000 Kuala Pilah,
Negeri Sembilan, Malaysia
*Corresponding author (e-mail: wan_elina@uitm.edu.my)

Metal ions such as iro(III) ion (Fe^{3+}) have an impact on human health and also play an important function in biological systems. However, the negative effects of Fe^{3+} ion to human and environment motivate the researchers to find a simple and quick method for Fe^{3+} detection. The aim of this study is to develop a simple method for determination of Fe^{3+} ion using Alizarin Red S (ARS) reagent. The reaction between ARS and Fe^{3+} ion has produced ARS-Fe(III) blackish-brown complex. All the optimization studies were carried out using UV-Vis Spectrophotometer at 572 nm. A dynamic linear range in acetate buffer solution was obtained in the range of 0.02 - 0.25 M with R^2 value of 0.9909. Moreover, stability study indicated that ARS showed stable response for about 7 hours while the reproducibility study was found to give a satisfactory relative standard deviation (RSD) value of 1.63 % and 0.85 %. Based on the interference study, Al^{3+} and Ca^{2+} were found to not significantly interfere in the detection of Fe^{3+} ion while Cu^{2+} showed some interference. This proposed method is deemed simple and could be a promising method for a rapid and direct detection of Fe^{3+} ion in both qualitative and quantitative approaches.

Keywords: UV-Vis spectrophotometer; iron (III); Alizarin Red S; optical sensor

Received: November 2023; Accepted: February 2024

Industrial activity-related environmental pollution is becoming a major issue that threatens both human health and ecosystems worldwide. Heavy metal ions and organic compounds make up the majority of the contaminants in industrial wastewater [1]. Heavy metal ions are more difficult to break than organic substances and can quickly accumulate in plants and animals. In addition, the ecosystem and biological health are severely harmed by the high toxicity of heavy metal ions [2]. Although iron(III), Fe^{3+} ions are one of the most prevalent heavy metal ions in industrial wastewater, its negative effects have not received adequate attention for a long time [3].

Depending on the concentration, Fe^{3+} ion have an impact on human health and play important functions in biological systems [4]. Fe^{3+} ion plays an important part in physiological activities like oxygen absorption, oxygen metabolism, and electron transport. In addition, the World Health Organization (WHO), Environmental Protection Agency (EPA) of the United States and Engineering Services Department of the Ministry of Health Malaysia has set 5.36 µM as the maximum allowable level of Fe^{3+} ion in drinking water [2, 5, 6]. Meanwhile, the European Union specifies 3.57 µM as the maximum allowable concentration of Fe^{3+} ion in drinking water [7]. Excessive levels of Fe^{3+} can cause a number of illnesses, such as immune system deterioration, kidney and liver damage, anaemia, heart failure, insufficient oxygen supply, and low blood pressure [8-9]. Additionally, too much Fe^{3+} ion can result in the production of reactive oxygen species (ROS), which can seriously harm an organism. Reactive oxygen species are frequently distinguished by their extraordinary capacity to cause damage to biomolecules such as protein, lipids, and nucleic acids [10].

One of the most crucial areas of analytical chemistry are detection of heavy metal ions in environmental samples [11-12]. Many analytical chemists are very interested in developing extremely effective chelating agents that are sensitive, and selective for the identification of heavy metals. Over the past few decades, numerous methods have been used to detect metals ion such as flame atomic absorption spectrometry [13-14] and spectrophotometry methods [15-16]. Both flame atomic absorption spectrometry and spectrophotometry methods are the common detection methods that rely on sophisticated equipment. However, this method requires sample preparation step and time consuming.

Hence, it is very essential to develop alternative and simple methods for detecting Fe^{3+} ions as these heavy metal ions have become a global issue especially on water pollution. Water contains Fe^{3+} ions, which progressively becomes more harmful inside the human body. On top of that, Fe^{3+} ions are not biodegradable

---

†Paper presented at the 3rd Virtual International Symposium on Sciences (3rd VISoS 2023)

in nature and that may cause accumulation in soil and human body [17]. Most of the current researches on Fe^{3+} ion detection are based on fluorescence method [18-22]. Xiang et al. [18] used carbon dot for detection of Fe^{3+} ion with excellence selectivity while Shahat et al. [19] used mesoporous silica nanotubes (MSNTs) for detection of Fe^{3+} ion where the sensor could be used for about 8 times. In their study, there was a colour change that could be observed with the naked eye after reacting with Fe^{3+} ion, however, the synthesis of sensing agent involved a complicated and time-consuming process. In the study by Xiang et al. [18], the sensor did not involve any colour change and it also involved a time-consuming synthesis process. Study by Rishabh et al. [20], Benny et al. [21], and Cheng et al. [22] involved the synthesis of carbon dots for detection of Fe^{3+} ion through fluorescence approach.

Spectrophotometry is a simple, quick, and less costly than the other methods [23]. Thus, in this study, we attempted to develop a new and simple spectrophotometric method for the detection of Fe^{3+} ions that employed Alizarin Red S (ARS) as the indicator. The suitability of the ARS as sensing agent for determining Fe^{3+} ion had also been investigated by conducting the optimization and evaluation of the analytical performance between Fe^{3+} ion and ARS. This method is considered very simple, rapid, cheap, and easy to develop as there are less chemicals involved.

EXPERIMENTAL

Chemicals and Materials

All reagents were of analytical reagent grade. iron(III) chloride hexahydrate (HmbG Chemicals), Alizarin Red S (R&M Chemicals), sodium acetate anhydrous (99%, R&M Chemicals), glacial acetic acid (R&M Chemicals), calcium chloride (R&M Chemicals), aluminium chloride 6-hydrate (Sigma Aldrich) and copper (II) nitrate trihydrate (R&M Chemicals) were used. De-ionized water was used throughout the experiment.

Instrumentations

The instruments used were T80/T80+ Double Beam UV-Vis spectrophotometer (PG Instruments Limited), analytical balance, hot plate, and pH meter.

Preparation of ARS Stock Solution

Alizarin Red S (ARS) stock solution 0.01 M was prepared by weighing 0.0360 g of ARS and dissolving in deionized water in a 100 ml volumetric flask until the calibration mark.

Preparation of Fe^{3+} Ion Stock Solution

Iron (III) stock solution was prepared by weighing 81.099 g of iron (III) chloride hexahydrate ($FeCl_3$. $6H_2O$) and dissolving with deionized water in a 100 ml volumetric flask until the calibration mark.

Preparation of Acetate Buffer Solution

Acetate buffer solution 0.1 M was prepared by weighing 4.1015 g of sodium acetate anhydrous ($C_2H_3NaO_2$) and dissolving with deionized water in a 500 ml volumetric flask until the calibration mark. Then, $C_2H_3NaO_2$ solution and a few drops of glacial acetic acid (CH_3COOH) were mixed together to prepare pH 3 until 5.

Optimization

All the optimization studies were carried out using UV-Vis spectrophotometer.

Absorption Spectrum of ARS, Fe^{3+} Ion and ARS-Fe(III) Complex

For measuring the absorption spectrum of ARS, Fe^{3+} ion and ARS-Fe complex, both ARS and Fe^{3+} with concentration of 3.5×10^{-4} M and 0.37 M were used. For the preparation ARS-Fe complex, about 0.35 ml of ARS from 0.01 M stock solution and 1.23 ml of Fe^{3+} from 3 M stock solution were mixed together. The spectra of ARS, Fe^{3+} ion and ARS-Fe complex were recorded from 300 nm until 750 nm using UV-Vis spectrophotometer.

Effect of pH

For the determination of optimum pH for the ARS-Fe(III)complex, acetate buffer was used. The concentration of ARS and Fe^{3+} ion used were 3.5×10^{-4} M and 0.2 M, respectively. The absorbance of ARS-Fe(III) complex was measured in the pH range of 3 to 5 using 0.1 M acetate buffer. Plot of absorbance at 572 nm versus pH was plotted.

Effect of ARS Concentration

In this study, different ARS concentrations (5.0×10^{-5} M until 3.0×10^{-4} M) were prepared individually in 10 ml volumetric flask by mixing an appropriate amount of 0.01 M ARS stock solution, 0.2 M Fe^{3+} ion solution and 2 ml acetate buffer solution pH 4. The plot of absorbance versus ARS concentration was plotted.

Effect of Fe^{3+} ion Concentration

Different Fe^{3+} ion concentrations (2.5×10^{-4} to 1.5 M) were prepared individually in 10 ml volumetric flask by mixing an appropriate amount of 3 M Fe^{3+} stock solution, 0.25 mL of 2.5×10^{-4} M ARS solution, 2 ml of acetate buffer solution pH 4 into a 10 ml volumetric flask and the deionized water was added until the calibration mark. The plot of absorbance versus Fe^{3+} ion concentration was plotted.

Stability Study

Stability study was conducted to determine ARS stability when exposed to light for a longer period of time. ARS solution with concentration of 2.5 x 10^{-4} M and 4.0 x 10^{-4} M were prepared from 0.01 M stock solution. The preparation of the solution was carried out in a 50 ml volumetric flask and the absorbance was recorded using UV-Vis spectrophotometer for every 1 hour for the duration of 7 hours. The relative standard deviation (RSD) was calculated and the plot of absorbance versus time was plotted.

Reproducibility Study

Reproducibility study was conducted at two Fe^{3+} ion concentrations which are 5.0 x 10^{-4} M and 0.25 M. The reaction between ARS and 5.0 x 10^{-4} M Fe^{3+} and 0.25 M Fe^{3+} were carried out in acetate buffer solution pH 4. The same steps were carried out eight times. The relative standard deviation (RSD) value was calculated and the graph of absorbance versus number of measurements was plotted.

Interference Study

Interference study was carried out to test whether the presence of other ions can interfere with the determination of Fe^{3+} ion. In this study, several kinds of cation comprised of Al^{3+}, Cu^{2+} and Ca^{2+} were chosen to determine the level of interference to the Fe^{3+} ion analysis. Interference studies were carried out by mixing an appropriate amount of 1 M Fe^{3+} ion stock solution, 0.25 mL of 2.5 x 10^{-4} M ARS solution and 2 ml of acetate buffer solution pH 4 into a 10 ml volumetric flask and the deionized water was added until the calibration mark. The same step was repeated for Al^{3+}, Ca^{2+}, and Cu^{2+} ions and the absorbances were recorded using UV-Vis spectrophotometer.

In addition, the absorbance of Fe^{3+} ion with the presence of Al^{3+} ion was measured by using a mixture of 1:1 and 1:2 (interfering species: Fe^{3+} ion). The mixture of 0.5 and 1.0 M Fe^{3+} ion solution with Al^{3+} ion solution (0.5 M and 1.0 M), 0.01 M ARS stock solution, and 2 ml of acetate buffer solution pH 4 was added into a 10 ml volumetric flask and the solution was diluted with deionized water until calibration mark. The same step was repeated for Ca^{2+} and Cu^{2+} ions solution. All the measurements were repeated for three times and the graph of absorbance versus interference species was plotted. The t-test statistical analysis was carried out to identify whether there was any significant difference between the absorbance of Fe^{3+} ion and interference species by using the equation below:

$$t = \frac{m - \mu}{s/\sqrt{n}}$$

Where:
m = mean
µ = theoretical value
s = standard deviation
n = variable set size

RESULTS AND DISCUSSION

Absorption Spectrum of ARS, Fe^{3+} Ion and ARS-Fe(III) Complex

Alizarin Red S (ARS) was used for detection of many metals and well-known analytical reagents for both qualitative and quantitative metal analysis. Figure 1 illustrate the UV-Vis spectra for ARS, Fe^{3+} ion and ARS-Fe(III) complex where the maximum wavelength of ARS and Fe^{3+} appears at 422 nm and 489 nm, respectively. Before reaction with Fe^{3+} ion solution,

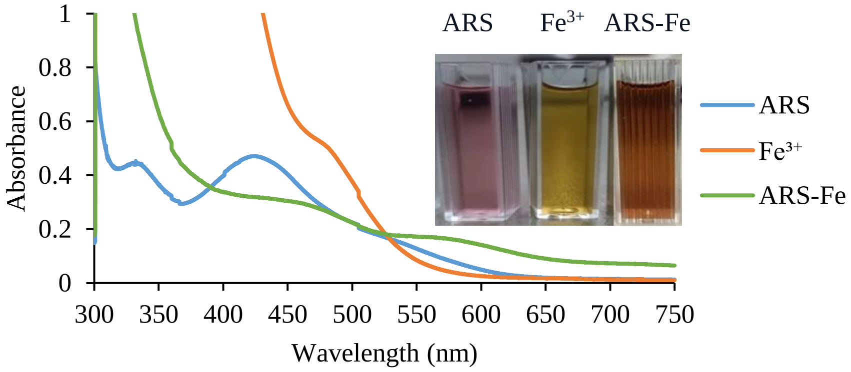

Figure 1. ARS, Fe^{3+} ion and ARS-Fe(III) complex spectra at Fe^{3+} and ARS concentration of 0.37 M and 3.5 x 10^{-4} M, respectively. Inset: The colour of ARS, Fe^{3+} and ARS-Fe(III) complex solution.

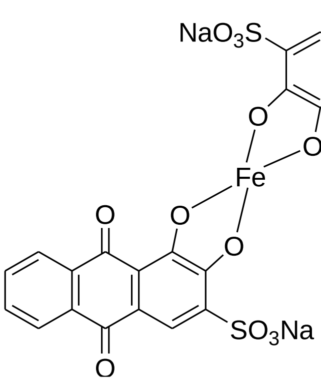

Figure 2. The chemical structure of the expected ARS-Fe(III) complex.

ARS powdered was brownish-yellow in colour and the colour changed to blackish-brown when it reacted with Fe^{3+} ion solution [24]. The reaction between ARS and Fe^{3+} displayed a bathochromic shift from 422 nm to 572 nm [25]. Figure 2 shows the expected ARS-Fe(III) complex structure when Fe^{3+} ion reacted with ARS where it was expected to bind through oxygen atom in ARS [26].

Effect of pH

The effect of pH was carried out to determine the optimum pH for the complete reaction between ARS and Fe^{3+} ion to produce ARS-Fe(III) complex. ARS-Fe(III) complex form a reddish-brown colour in the presence of acetate buffer due to formation of $[Fe_3(OH)_2(CH_3COO)_6]^+$. Figure 3 illustrates the UV-Vis absorbance plot of ARS-Fe(III) complex in acetate buffer pH 3 until 5. Based on the finding, the highest absorbance occurred at pH 4.0 and this pH was considered the optimum pH for the reaction between ARS and Fe^{3+} solution. The finding are consistent with the previous study by Biesuz et al. [27]. Biesuz et al. [27] in their research on sorption of Fe^{3+} on ARS-Colour Catcher (Aliz-CC) stated that the complex of ARS and Fe^{3+} formed a stable complex at pH 4.5. In a study by Das et al. [28], it was observed that the complex formation of rhodamine-6G (L^2) with Fe^{3+} ions exhibited a decreasing trend in fluorescence response within the pH range of 7 to 8. ARS-Fe(III) complex solution was found to form precipitate and became cloudy at pH greater than 5 or lower than 3.

Effect of ARS Concentration

This study was carried out to determine the optimum concentration for the ARS-Fe(III) complex. For the effect of ARS concentration, the absorbance of ARS was found to increase with the increasing of ARS concentration as postulated by Beer-Lambert Law (Figure 4). Beer-Lambert Law is applicable only for analyte with a lower concentration [29]. In this study, 2.5 x 10^{-4} M has been chosen as the optimum concentration and the concentration was used for the next study. This was due to the absorbance value of less than 1 which indicated 90% absorption of light [30].

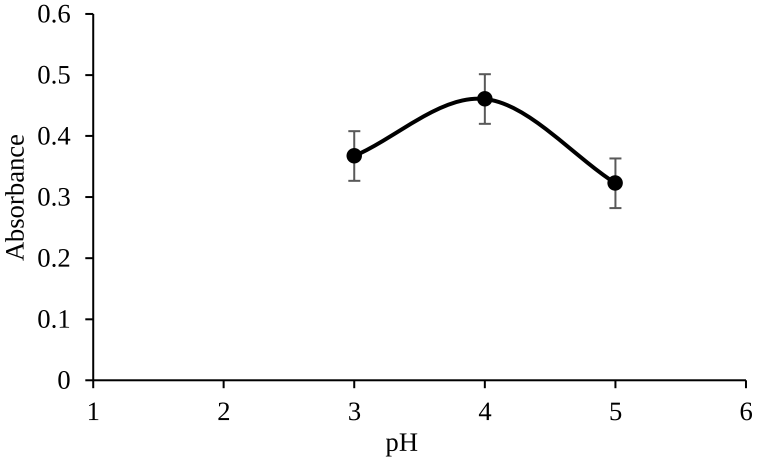

Figure 3. Plot of absorbance versus pH (pH 3 until 5) by using acetate buffer. The measurement was recorded at wavelength of 572 nm with the concentration of ARS and Fe^{3+} ion used were 3.5 x 10^{-4} M and 0.2 M, respectively.

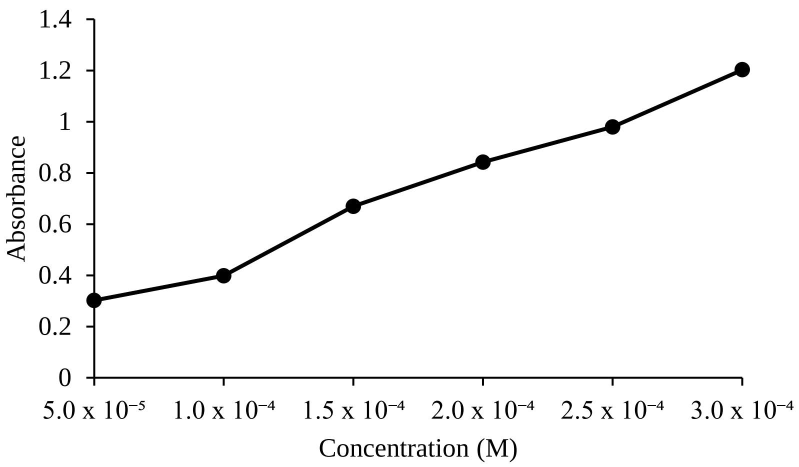

Figure 4. Plot of absorbance versus ARS concentration (5.0 x 10^{-5} M to 3.0 x 10^{-4} M) reacted with 0.2 M Fe^{3+} ion in acetate buffer pH 4. The measurement was recorded at wavelength of 572 nm.

Effect of Fe^{3+} Ion Concentration

The effect of different concentration of Fe^{3+} was determined by measuring the absorbance of ARS-Fe(III) complex at different concentration of Fe^{3+} from 2.5 x 10^{-4} to 1.5 M (Figure 5). There was an increasing trend in the absorbance with the increasing of Fe^{3+} ion concentration at 572 nm. The increasing trend are due to the Beer-Lambert Law in which it states that absorbance is directly proportional to the concentration [31]. A linear response was found in the range of 0.02 - 0.25 M with R^2 value of 0.9909 (Figure 6). Further increase in the Fe^{3+} ion concentration showed that the absorbance signal gave a plateau region. The point indicated that all the ARS had been used for the reaction with Fe^{3+} ion [32].

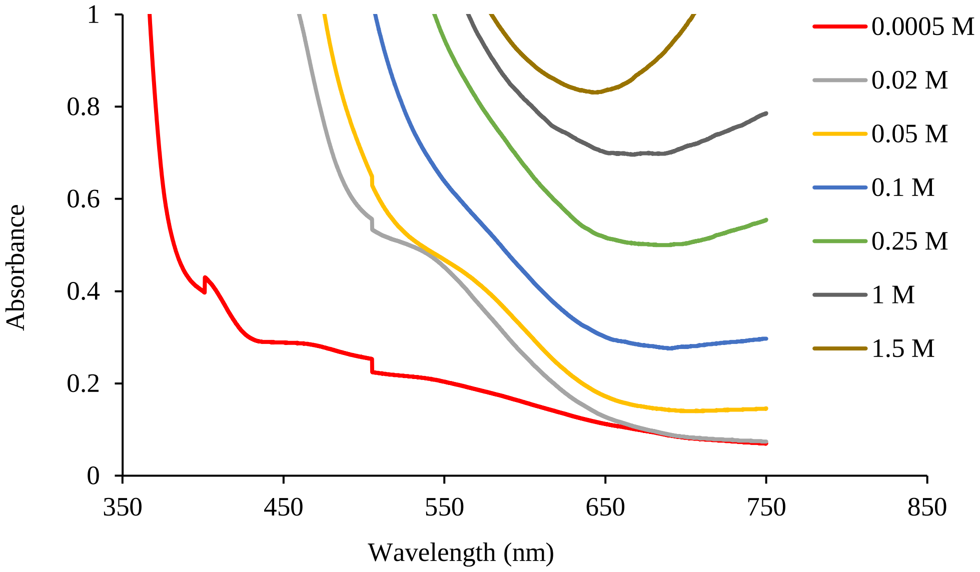

Figure 5. Absorption spectra of ARS-Fe(III) complex solution with different concentrations of Fe^{3+} ion (2.5 x 10^{-4} to 1.5 M) and ARS concentration fixed at 2.5 x 10^{-4} M in acetate buffer pH 4.

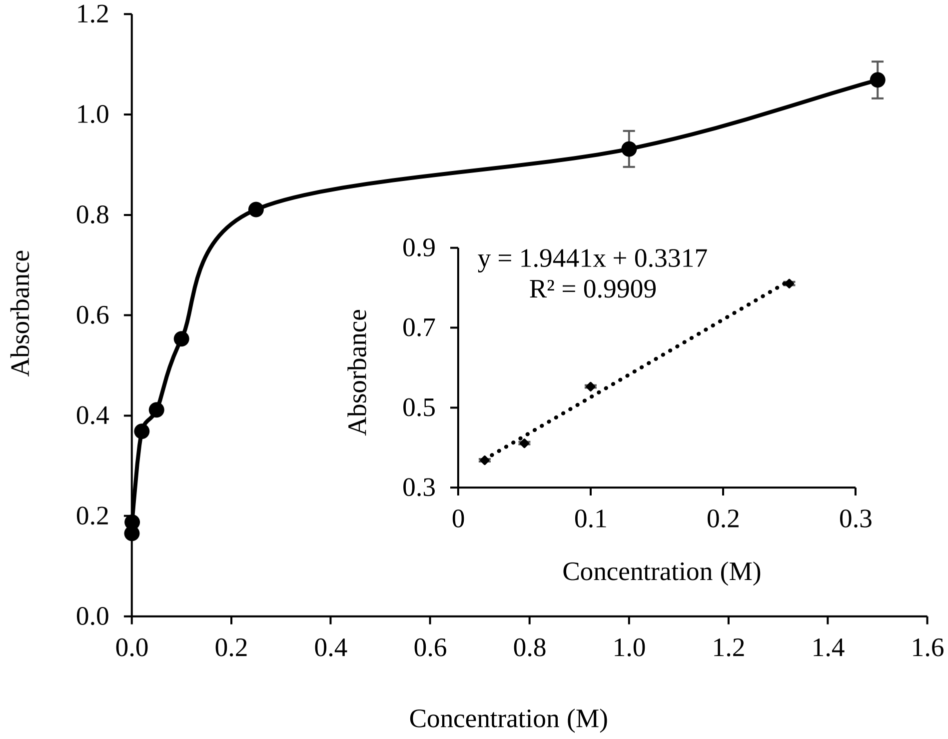

Figure 6. Plot of absorbance versus Fe^{3+} ion concentration (2.5 x 10^{-4} to 1.5 M) reacted with 2.5 x 10^{-4} M ARS in acetate buffer pH 4 at 572 nm. Inset: Plot of absorbance versus Fe^{3+} ion concentration in the range of 0.02 - 0.25 M reacted with 2.5 x 10^{-4} M ARS in acetate buffer pH 4 at 572 nm.

Stability Study

This study was carried out to identify the stability of ARS reagents. Stability studies were carried out using 2.5 x 10^{-4} M and 4.0 x 10^{-4} M ARS solution. The stability of the ARS solution was analysed every 1 hour for the duration of 7 hours (Figure 7). The relative standard deviation (RSD) obtained were 0.54% and 2.85% for 2.5 x 10^{-4} M and 4.0 x 10^{-4} M ARS, respectively. The RSD values indicated that the ARS was stable when it was exposed to the light source for at least 7 hours [25].

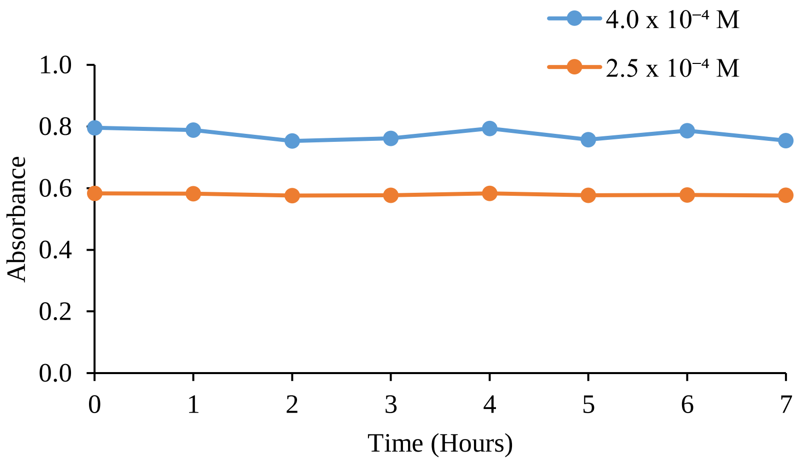

Figure 7. Plot of absorbance versus time for stability study of 4.0 x 10^{-4} M and 2.5 x 10^{-4} M ARS for the duration of 7 hours.

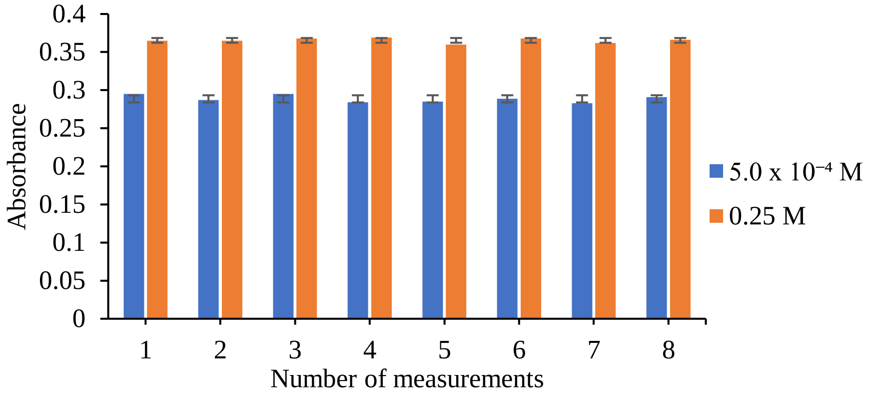

Figure 8. Absorbance plot of ARS-Fe(III) complex at a fixed ARS concentration of 2.5 x 10^{-4} M with Fe^{3+} ion concentration both at 5.0 x 10^{-4} M and 0.25 M in acetate buffer pH 4 at 572 nm.

Reproducibility Study

The reproducibility study was carried out by measuring the absorbance of 10 trials of ARS-Fe(III) complex at the same concentration (Figure 8). Based on the calculation, ARS-Fe(III) complex yield the relative standard deviation (RSD) of 1.63% and 0.85% for Fe^{3+} ion concentration of 5.0 x 10^{-4} M and 0.25 M, respectively. The RSD value less than 5% signified that the measurements was consistent and the reproducibility of the method was good since the data points tended to be extremely near to the mean [33].

Interference Study

Interference study was conducted to identify any common species that are present in the water that may interfere with the detection of Fe^{3+} ion. The common species that can be found in water are Al^{3+}, Ca^{2+}, and Cu^{2+} ions and they have been chosen for this study [5, 34]. Generally, the peak and absorbance of the ARS-Fe(III) complex at 572 nm may be influenced by the presence of potential interfering species. Figure 9 illustrate the absorbance of ARS-Cu complex that shows the highest signal as compared to other possible interfering species. The interference from Cu^{2+} ion was expected due to the ARS capability to form a complex with Cu^{2+} [35].

In order to test whether there were any significant differences between the absorbance value of the ARS-Fe(III) complex with the other interference species, t-test statistical analysis was performed. A p-values that are less than 0.05 show that there is a significant difference between the absorbance value of ARS-Fe(III) complex and ARS-interfering complex [36]. The p-values of ARS-Al (III) and ARS-Ca(II) complexes were less than 0.05 which meant that there was a significant difference between the ARS-Al and ARS-Ca complexes with ARS-Fe(III) complex thus accepting the null hypothesis (Table 1). The difference in the absorbance of ARS-Fe(III) complex with ARS-Al(III) and ARS-Ca(II) complexes showed that Al^{3+} and Ca^{2+} ions had not interfered with the absorbance of ARS-Fe(III) complex. Although the p-value of ARS-Cu complex was also less than 0.05, it was still considered to have interfered with detection of Fe^{3+} ion because the absorbance value of ARS-Cu was close to the absorbance of ARS-Fe(III) complex.

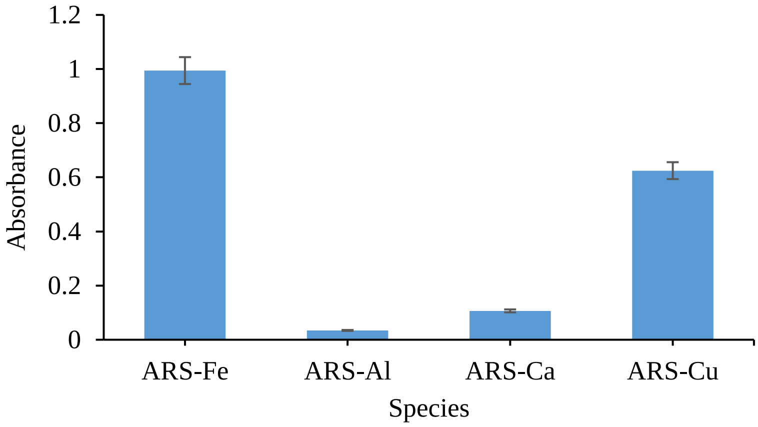

Figure 9. Interference study at interfering species concentration of 1.0 M. The measurement was recorded in acetate buffer solution pH 4 at 572 nm.

Table 1. p-value of ARS-interference complex in comparison with ARS-Fe(III) complex at 572 nm.

Species	p-value
ARS-Al(III)	3.1912×10^{-10}
ARS-Ca(II)	8.6064×10^{-10}
ARS-Cu(II)	6.9301×10^{-7}

Table 2. Percentage of interference for the Al^{3+}, Ca^{2+} and Cu^{2+} ions at wavelength of 572 nm.

Metal	% Interference (1:1)	% Interference (1:2)
ARS-Al-Fe	-65.69	-52.92
ARS-Ca-Fe	-53.82	-38.43
ARS-Cu-Fe	-25.75	-13.58

Note: Interference (%) = ((x-y)/y) x 100, where x is the absorbance value for mixed solution of Fe^{3+} and interfering species, y is the absorbance value for Fe^{3+} solution only [19].

The interference study was also carried out by mixing Fe^{3+} ion and interfering species and the absorbance in the presence and absence of interfering species were recorded. The analysis was conducted at two concentration ratio which were 1:1 and 1:2 (interfering species: Fe^{3+} ion). Table 2 show the percent interference for ARS-Al-Fe, ARS-Ca-Fe and ARS-Cu-Fe at two concentrations ratios which are 1:1 and 1:2. Positive interference happens when an interference ion reacts with a reagent to create a species with a higher intensity colour. Negative interferences are caused by an incomplete reaction between the interference ion and the analyte [32]. Based on Table 2, percent interference for all the possible interfering species exceeded 5%.

It is evident from Table 2 that Al^{3+} and Ca^{2+} ions exert significant interference on the determination of Fe^{3+} ions, with Al^{3+} exhibiting the highest percentage of interference. This interference is primarily attributed to the ability of Al^{3+} and Ca^{2+} ions to react with ARS [25]. However, the interference can be lessened by incorporating citric acid as a masking agent [37]. Citric acid is known for its high selectivity and affinity for binding Al^{3+} [38], thereby reducing interference effects.

CONCLUSION

A simple and rapid spectrophotometric method has been developed for detection of Fe^{3+} ion by using ARS reagent. The chemical interaction of ARS and Fe^{3+} ion produce ARS-Fe(III) complex that showed one prominent peak at 572 nm. The ARS solution underwent a colour change from red to blackish-brown when it formed complex with Fe^{3+} ion. The determination of Fe^{3+} ion was linear in acetate buffer pH 4 in the range of 0.02-0.25 M with R^2 value of 0.9909. The ARS-Fe(III) complex formation showed a good reproducibility with RSD value of 0.85 - 1.63 %. The interference study showed that the other cations such as Al^{3+} and Ca^{2+} had interfered with detection of Fe^{3+} ion.

ACKNOWLEDGEMENTS

The authors would like to thank the School of Chemistry and Environment, Universiti Teknologi MARA Cawangan Negeri Sembilan (UiTMCNS) and Microbiology Laboratory UiTMCNS for providing the research facilities to carry out the work.

REFERENCES

1. Fan, J., Kang, L., Cheng, X., Liu, D. and Zhang, S. (2022) Biomass-derived carbon dots and their sensing applications. *Nanomaterials*, **12**, 1–25.

2. Kang, S., Han, H., Lee, K. and Kim, K. M. (2022) Ultrasensitive detection of Fe^{3+} ions using functionalized graphene quantum dots fabricated by a one-step pulsed laser ablation process. *ACS Omega*, **7(2)**, 2074–2081.

3. Wang, R. D., Zhang, W. Q., Zhou, S., Tang, J., He, M., Zhang, S., Du, L. and Zhao, Q. H. (2022) A novel dual-functional coordination polymer for detection and ultra-effectively removal of Fe(III) in water. *Journal of Molecular Liquids*, **355**, 1–10.

4. Rojas-Romo, C., Aliaga, M. E., Arancibia, V. and Gomez, M. (2020) Determination of Pb(II) and Cd(II) via anodic stripping voltammetry using an in-situ bismuth film electrode. Increasing the sensitivity of the method by the presence of

Alizarin Red S. *Microchemical Journal*, **159**, 1–10.

5. Ji, W., Zhu, Z., Dong, S., Nie, J. and Du, B. (2019) Optical detection of Fe^{3+} ions in aqueous solution with high selectivity and sensitivity by using sulfasalazine functionalized microgels. *Sensors*, **19**, 1–14.

6. Engineering Services Division Ministry of Health Malaysia (2004) National standard for drinking water quality. *Ministry of Health Malaysia*, **2**, 1–26.

7. Xiang, Z., Jiang, Y., Cui, C., Luo, Y. and Peng, Z. (2022) Sensitive, selective and reliable detection of Fe^{3+} in lake water via carbon dots-based fluorescence assay. *Molecules*, **27(19)**, 1–12.

8. Chantarasunthon, K., Promkatkaew, M., Waranwongcharoen, P., Sueksachat, A., Prasop, N., Norasi, T., Sonsiri, N., Sansern, S., Chomngam, S., Wechakorn, K., Thana, C., Sakulsaknimitr, W., Kongsaeree, P. and Srisuratsiri, P. (2023) A novel highly selective FRET sensor for Fe(III) and DFT mechanistic evaluation. *Spectrochimica Acta - Part A: Molecular and Biomolecular Spectroscopy*, **286**, 1–7.

9. Gupta, M. and Lee, H. Il. (2019) Water-soluble polymeric probe with dual recognition sites for the sequential colorimetric detection of cyanide and Fe(III) ions. *Dyes and Pigments*, **167**, 174–180.

10. Yang, M., Ahmed, H., Wu, W., Jiang, B. and Jia, Z. (2018) Cytotoxicity of air pollutant 9, 10 - phenanthrenequinone: Role of reactive oxygen species and redox signaling. *BioMed Research International*, **2018**, 1–15.

11. Tian, M., Fang, L., Yan, X., Xiao, W. and Row, K. H. (2019) Determination of heavy metal ions and organic pollutants in water samples using ionic liquids and ionic liquid-modified sorbents. *Journal of Analytical Methods in Chemistry*, **2019**, 1–19.

12. Malik, L. A., Bashir, A., Qureashi, A. and Pandit, A. H. (2019) Detection and removal of heavy metal ions: a review. *Environmental Chemistry Letters*, 1–27.

13. Ghaedi, M., Mortazavi, K., Montazerozohori, M., Shokrollahi, A. and Soylak, M. (2013) Flame atomic absorption spectrometric (FAAS) determination of copper, iron and zinc in food samples after solid-phase extraction on Schiff base-modified duolite XAD 761. *Materials Science and Engineering C*, **33**, 2338–2344.

14. Soylak, M. and Aydin, A. (2011) Determination of some heavy metals in food and environmental samples by flame atomic absorption spectrometry after coprecipitation. *Food and Chemical Technology*, **49**, 1242–1248.

15. Taha, S. S., Ali, D. S., Hassan, R. O., Othman, H. O. and Smaoui, S. (2023) Colorimetric and fluorescent dual mode detection of Fe (III) ion in blood samples in combination with cloud point extraction. *Microchemical Journal*, **195**, 109390.

16. Moghadam, M. R., Haji Shabani, A. M. and Dadfarnia, S. (2011) Spectrophotometric determination of iron species using a combination of artificial neural networks and dispersive liquid–liquid microextraction based on solidification of floating organic drop. *Journal of Hazardous Materials*, **197**, 176–182.

17. Arvapalli, D. M., Sheardy, A. T., Alapati, K. C. and Wei, J. (2020) High quantum yield fluorescent carbon nanodots for detection of Fe(III) ions and electrochemical study of quenching mechanism. *Talanta*, **209**, 1–9.

18. Xiang, Z., Jiang, Y., Cui, C., Luo, Y. and Peng, Z. (2022) Sensitive, selective and reliable detection of Fe^{3+} in lake water via carbon dots-based fluorescence assay. *Molecules*, **27**, 6749.

19. Shahat, A., Elamin, N. Y. and Wesam Abd El-Fattah, W. (2022) Spectrophotometric and fluorometric methods for the determination of Fe(III) ions in water and pharmaceutical samples. *ACS Omega*, **7**, 1288−1298.

20. Rishabh., Rani, M., Shanker, U., Kaith, B. S. and Sillanpa, M. (2024) Green fabrication of fluorescent N-doped carbon quantum dots from *Aegle marmelos* leaves for highly selective detection of Fe^{3+} metal ions. *Inorganic Chemistry Communications*, **159**, 111878.

21. Benny, A., Joemol, P. G., Sajeevan, A. and Thomas, T. S. Green synthesis and characterization of carbon dots from *Angiopteris evecta* (G.Forst.) Hoffm and selective detection of Fe^{3+} ions. *Materials Today: Proceedings*. (article in press).

22. Cheng, Z. -F., Wu, X. -Y., Liu, L., He, L., Yang, Z. Y., Cao, C., Lu, Y. and Guo, J. X. (2023) A highly efficient, rapid, room temperature synthesis method for coal-based water-soluble fluorescent carbon dots and its use in Fe^{3+} ion detection. *New Carbon Materials*, **38(6)**, 1104–1115.

23. Campbell, D., Pethrick, R. A. and White, J. R. (2000) *Polymer Characterization, CRC Press.*

24. Gahlan, A. A., El-Mottaleb, M. A., Badawy, N. A., Kamale, F. H. and Ali, S. H. (2014) Spectrophotometeric studies on binary and ternary complexes of some metal ions with alizarin red s and cysteine. *International Journal of Advanced Research,* **2(10)**, 570–584.

25. Supian, S. M., Ling, T. L., Heng, L. Y. and Chong, K. F. (2013) Quantitative determination of Al(III) ion by using alizarin red s including its microspheres optical sensing material. *Analytical Methods*, **5**, 2602–2609.

26. Moriguchi, T., Nakagawa, S. and Kaji, F. (2010) Adsorbability of alizarin red s on Fe(III) and Pb(II) treated hydroxyapatites in water. *Phosphorus Research Bulletin*, **24**, 62–72.

27. Biesuz, R., Nurchi, V. M., Magnaghi, L. R. and Alberti, G. (2019) Inexpensive alizarin red s-based optical device for the simultaneous detection of Fe(III) and Al(III). *Microchemical Journal*, **149**, 1–7.

28. Das, D., Alam, R., Sasmal, M., Katarkar, A., Dutta, A. and Ali, M. (2024) A rhodamine-6G based chromo and fluorogenic sensor for the selective turn-ON detection of Fe^{3+} in aqueous medium with potential applications as INHIBIT logic gate, memory device and live cell imaging. *Inorganica Chimica Acta*, **563**, 121902.

29. Cerdà, V., Phansi, P. and Ferreira, S. (2022) From mono- to multicomponent methods in UV-VIS spectrophotometric and fluorimetric quantitative analysis - A review. *Trends in Analytical Chemistry*, **157**, 116772.

30. Thiha, A. and Ibrahim, F. (2015) A colorimetric enzyme-linked immunosorbent assay (ELISA) detection platform for a point-of-care dengue detection system on a lab-on-compact-disc. *Sensors*, **15**, 11431–11441.

31. Delgado, R. (2021) Misuse of Beer–Lambert Law and other calibration curves. *Royal Society Open Science*, **9**, 211103.

32. Wan, K. W. E. F., Ahmad, M. and Heng, L. Y. (2014) Characterization of a simple optical chemical sensor for Cu(II) detection based on immobilization of lipophilized nitroso-r reagent in sol-gel matrix. *Chiang Mai Journal of Science*, **41(2)**, 383–394.

33. Taylor, J. K. (1983) Validation of analytical methods. *Analytical Chemistry*, **55(6)**, 600A–608A.

34. Kim, K., Nam, Y. S., Lee, Y. and Lee, K. B. (2017) Highly sensitive colorimetric assay for determining Fe^{3+} based on gold nanoparticles conjugated with glycol chitosan. *Journal of Analytical Methods in Chemistry*, **2017**, 1–11.

35. Raja Zaidatul Akhmar Raja Jamaluddin, Musa Ahmad, Heng, L. Y. and Tan, L. L. (2023) Filem mikrosfera akrilik terpegun alizarin merah s untuk pengesanan pendarfluor optik asid borik. *Sains Malaysiana*, **52(5)**, 1407–1417.

36. Mohd Fadli, M. E. I., Wan Khalid, W. E. F. and Abu Hanifah, S. (2023) Effect of interference study on carrageenan detection using ultraviolet visible spectrophotometry. *Sains Malaysiana*, **52(6)**, 1711–1721.

37. Peng, L., Guo, H., Wu, N., Wang, M., Hao, Y., Ren, B., Hui, Y., Ren, H. and Yang, W. (2024) A dual-functional fluorescence probe CDs@ZIF-90 for highly specific detection of Al^{3+} and Hg^{2+} in environmental water samples. *Analytica Chimica Acta*, **1288**, 342171.

38. Köstereli, Z. and Severin, K. (2015) Selective detection of Al^{3+} and citric acid with a fluorescent amphiphile. *Organic & Biomolecular Chemistry*, **13**, 252